

Dilution Control in Gas-Tungsten-Arc Welds Involving Superaustenitic Stainless Steels and Nickel-Based Alloys

S.W. BANOVIC, J.N. DuPONT, and A.R. MARDER

Fusion welds were prepared between a superaustenitic stainless steel, (the AL-6XN alloy) and two Ni-based filler metals (IN625 and IN622) using the gas-tungsten-arc welding (GTAW) process. Fusion-zone compositions over the full range of dilution levels (0 to 100 pct) were produced by varying the independent welding parameters of arc power and volumetric filler-metal feed rate. Microstructural characterization of the welds was conducted *via* light optical microscopy, with quantitative chemical information obtained through electron-probe microanalysis (EPMA). The dilution level of each weld was determined from the EPMA data as well as through geometric measurements of the weld cross-sectional areas. The dilution level was observed to decrease with increasing filler-metal feed rate and decreasing arc power. These effects are quantitatively interpreted based on a previously proposed processing model. The model is used to demonstrate that, in terms of welding parameters, the dilution level can be correlated exclusively to the *ratio* of the volumetric filler-metal feed rate (V_{fm}) to arc power (VI), *i.e.*, the individual values of V_{fm} and VI are not important in controlling the dilution and resultant weld-metal composition. Good agreement is obtained between experimental and calculated dilution values using the model. It is also demonstrated that the melting enthalpies of the filler metal and substrate have only a minor influence on dilution at dilution levels in the range from 40 to 100 pct. This knowledge facilitates estimates of dilution levels in this range when the substrate and filler-metal thermal properties are not accurately known. The results presented from this study provide guidelines for controlling the weld-metal composition in these fusion-zone combinations.

I. INTRODUCTION

IN order to compensate for diminished mechanical or electrochemical properties in the fusion zone, the use of filler metals significantly different from that of the substrate composition have been considered in some joining applications. For example, this technique may find application in the welding of superaustenitic stainless steels, which have excellent corrosion resistance in the unwelded condition, but in which autogeneous welds are susceptible to localized corrosion attack. One such alloy is AL-6XN, which contains approximately 6 wt pct Mo for improved localized corrosion behavior (*i.e.*, pitting and crevice corrosion) in salt-water environments.^[1-4] However, recent work has shown that autogeneous welds in this alloy are susceptible to localized attack in the fusion zone when exposed to aggressive aqueous salt solutions.^[5,6] The areas preferentially attacked in the weld were identified as Mo-depleted dendrite cores, containing 4.5 wt pct Mo compared to 6.5 wt pct nominally, which developed during solidification as a result of microsegregation.^[5] Joining of AL-6XN with filler metals having a high Mo content, relative to the nominal content in AL-6XN, is often done to restore the weld-metal corrosion resistance.^[5] Two of these possible filler metals are the Ni-based IN625 and IN622 (8.5 and 14 wt pct Mo, respectively). These relatively high Mo filler metals are used to increase the Mo content of the dendrite cores to a level that provides improved corrosion resistance.

With this approach, the nominal and dendrite-core composition in the weld metal, as well as the concomitant corrosion resistance, will be controlled, to a large degree, by the dilution level. The dilution level, in turn, is strongly influenced by the welding parameters. Thus, any attempt to restore weld-metal corrosion resistance through "overalloyed" filler metals must also consider methods to control the dilution level through manipulation of the welding parameters. In view of these factors, a study was initiated to investigate the joining of AL-6XN with IN625 and IN622 alloys as the filler metals. Welds were systematically prepared using the two Ni-based alloys over a broad range of welding parameters, to provide the full spectrum of fusion-zone compositions that are possible in practical applications. This variation in weld-metal composition was accomplished by depositing welds under a wide range of filler-metal feed rates and arc powers and measuring the resultant weld-metal dilution. The deposited samples will further be used to evaluate the weldability and corrosion resistance of the weld material in companion articles. For this article, the focus will be on the processing of fusion welds prepared between AL-6XN and the Ni-based filler metals. The results from this study will provide a framework for controlling the weld-metal composition based on a knowledge of the welding parameters.

II. EXPERIMENTAL PROCEDURE

Bead-on-plate welds were produced using the gas-tungsten-arc welding (GTAW) process by directly feeding the filler metal into the weld pool of the substrate (Figure 1). With the nonconsumable-electrode GTAW process, the volumetric filler-metal feed rate (V_{fm}) and arc power (VI) can be independently controlled, thus easily changing the dilution levels. The substrate materials were approximately 0.64-cm

S.W. BANOVIC, Research Associate, J.N. DuPONT, Assistant Professor, and A.R. MARDER, Professor, are with the Department of Materials Science and Engineering, Lehigh University, Bethlehem, PA 18015.

Manuscript submitted February 1, 2001.

thick, 2.54-cm wide, and 15.25-cm long. The samples were held flush to the welding table in order to maintain a constant and reproducible heat sink, with the table being at room temperature (26 °C) before beginning each deposit. The travel speed was fixed at 2.0 mm/s with a 2.5 mm arc gap. Commercially pure argon was used as the shielding gas. To produce welds of various dilution levels, the processing parameters of the volumetric filler-metal feed rate and arc power were varied.

The materials used were AL-6XN and IN625, both in plate and filler-metal form. A small heat of IN622 filler metal was obtained, while the C-22 substrate (compositional equivalent for IN622) was used in plate form. Table I shows the respective compositions, as well as the diameters for the individual filler metals. In order to produce dilution levels from 0 to 100 pct, with respect to AL-6XN as the substrate, IN625 and IN622 filler metal was deposited on AL-6XN for high dilution levels, typically above 50 pct dilution. For the lower values, the materials were reversed, with AL-6XN filler metal being fed into the weld pools of the IN625 and C-22 substrates.

Samples were removed from the welds, mounted in cold-setting epoxy, and polished to a 0.04 μm finish with colloidal silica, using standard metallographic techniques. Higher-dilution-level samples were electrolytically etched in a mixture of nitric acid (HNO₃) and water (H₂O) in the proportions of 60/40, using a platinum cathode at a pre-set voltage of 5 V. For the lower dilution levels, 10 pct oxalic acid was used under the same conditions. Microstructural characterization was performed using light optical microscopy.

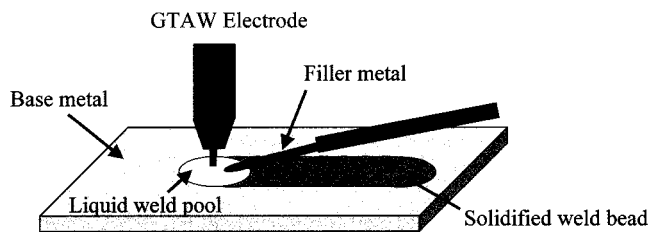


Fig. 1—Schematic of the GTAW process for producing the dissimilar metal welds.

Dilution levels were determined by two methods: chemical analysis and geometric dilution calculations. For the former, quantitative chemical information was obtained through use of an electron-probe microanalyzer (EPMA). A JEOL* 733 SuperProbe, equipped with wavelength-

*JEOL is a trademark of Japan Electron Optics Ltd., Tokyo.

dispersive spectrometers, was operated at an accelerating voltage of 15 kV and a probe current of 20 nA. Sampled areas were approximately 1500 μm², large enough to avoid any deviations that may be encountered due to microsegregation. The X-ray counts were converted to weight percentages using a ZAF correction scheme.¹⁷⁾ In the fully mixed fusion zone, the final weld composition will simply be a mixture of the substrate and filler metal:

$$C_{fz} = C_{fm}(1 - D) + C_s(D) \quad [1]$$

where C_{fz} , C_{fm} , and C_s are the elemental compositions of the fusion zone, filler metal, and substrate, respectively, and D is the dilution level. Thus, when C_{fz} , C_{fm} , and C_s are all known, the dilution level is simply determined by

$$D = \frac{C_{fz} - C_{fm}}{C_s - C_{fm}} \quad [2]$$

The values for the major constituents of Fe and Ni were used and averaged to get the final dilution level of the weld. Dilution levels were also determined using metallographic methods to measure the individual geometric cross-sectional areas of the deposited filler metal and melted substrate. The ratio of the melted substrate (A_s) to the total melted cross-sectional area from the filler metal and substrate ($A_s + A_{fm}$) is the dilution level (Figure 2):

$$D = \frac{A_s}{A_s + A_{fm}} \quad [3]$$

III. RESULTS

Sample matrices were produced to obtain a wide range of dilution levels for both sets of fusion welds between AL-6XN and IN625 or IN622. Filler-metal feed speeds between

Table I. Compositions for Raw Materials as Determined Using EPMA (Values under Compositions Are Standard Deviations)

| | Filler Metal Diameter | Fe | Ni | Cr | Mo | Nb | Mn | Si | Other |
|---------------|-----------------------|------|------|------|------|-----|-----|-----|-------|
| AL-6XN | | | | | | | | | |
| Filler metal | 0.064 in. | 47.6 | 23.9 | 21.3 | 6.1 | 0.0 | 0.2 | 0.3 | 0.8 |
| | | 0.7 | 0.5 | 1.1 | 0.4 | 0.0 | 0.1 | 0.1 | — |
| Plate | | 47.0 | 24.4 | 20.9 | 6.3 | 0.0 | 0.2 | 0.3 | 0.9 |
| | | 0.8 | 0.3 | 1.0 | 0.3 | 0.0 | 0.0 | 0.1 | — |
| IN625 | | | | | | | | | |
| Filler metal | 0.034 in. | 0.6 | 64.6 | 21.7 | 8.9 | 3.5 | 0.0 | 0.1 | 0.6 |
| | | 0.2 | 1.2 | 1.7 | 0.5 | 0.6 | 0.0 | 0.0 | — |
| Plate | | 4.5 | 60.8 | 20.8 | 8.7 | 3.5 | 0.1 | 0.2 | 1.4 |
| | | 0.3 | 0.9 | 1.1 | 0.7 | 0.4 | 0.0 | 0.0 | — |
| IN622 | | | | | | | | | |
| Filler metal | 0.035 in. | 2.4 | 59.0 | 20.5 | 14.3 | 0.0 | 0.2 | 0.0 | 3.4 |
| | | 0.1 | 1.8 | 0.7 | 0.6 | 0.0 | 0.0 | 0.0 | — |
| C-22 | | | | | | | | | |
| Plate | — | 3.6 | 56.7 | 21.3 | 13.2 | 0.0 | 0.2 | 0.0 | 5.0 |
| | | 0.2 | 1.5 | 1.1 | 0.5 | 0.0 | 0.0 | 0.0 | — |

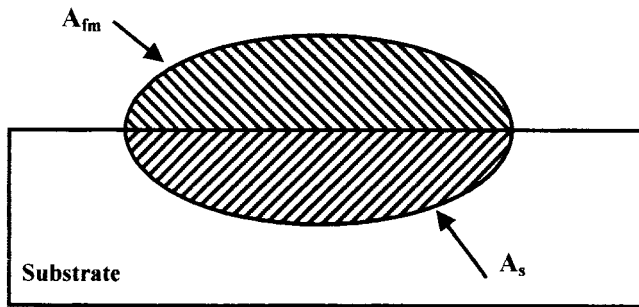


Fig. 2—Schematic illustration of the geometric measurements made for the dilution calculations using Eq. [3].

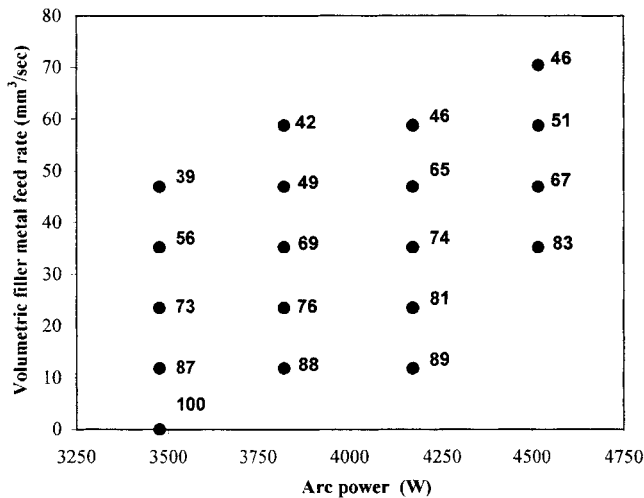


Fig. 3—Experimental matrix of fusion welds produced where AL-6XN was the substrate and IN625 was the filler metal. The numbers to the right signify the dilution level with respect to AL-6XN as the substrate.

0 and 120 mm/s were used, while the current (I) was varied between 250 and 325 A in 25 A increments, and voltages (V) averaged around 13.9 ± 1.3 V. This produced a range of arc powers from 3475 to 4520 W. Figures 3 and 4 display the experimental matrices produced for samples where AL-6XN was the substrate and IN625 and IN622 were the filler metals, respectively. The majority of experiments were conducted using the IN625 filler metal. Only selected parameter ranges were repeated for welds made with the IN622 filler metal. Due to the slightly different filler-metal diameters, the volumetric filler-metal feed rates varied slightly between the two graphs. Each data point represents a weld deposited at the specified volumetric filler-metal feed rate and arc power. The numbers located to the right of the symbols signify the resultant dilution levels determined by substituting EPMA measurements into Eq. [2]. Attempts were made to decrease the dilution level toward zero using AL-6XN as the substrate; however, a point was reached where the filler metal was not being completely melted and exited the weld pool still in solid form. Therefore, the full range of weld-metal compositions was obtained by reversing the materials during the process and depositing AL-6XN filler metal onto Ni-based substrates (Figures 5 and 6). In these two plots, the numbers located to the right of the symbols again signify the actual dilution levels obtained *via* chemical methods, while those to the left signify dilution levels with respect

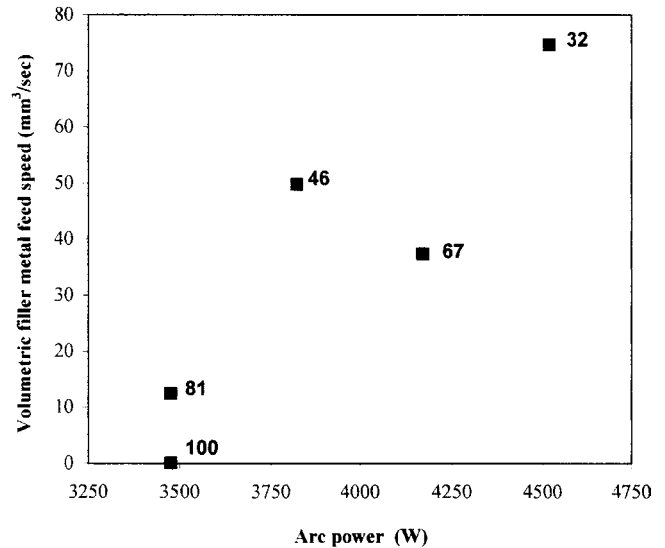


Fig. 4—Experimental matrix of fusion welds produced where AL-6XN was the substrate and IN622 was the filler metal. The numbers to the right signify the dilution level with respect to AL-6XN as the substrate.

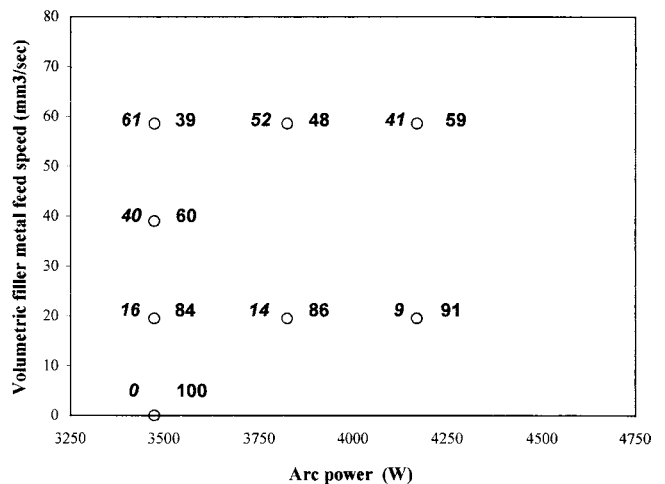


Fig. 5—Experimental matrix of fusion welds produced where IN625 was the substrate and AL-6XN was the filler metal. The numbers to the right signify the dilution level with respect to IN625 as the substrate, while those to the left are dilution levels with respect to AL-6XN as the substrate.

to AL-6XN as the substrate. Thus, these numbers are the actual dilution levels subtracted from 100. Relatively good agreement can be seen over the entire range of samples between the two methods used to calculate the dilution levels (Figure 7).

It should be noted that the dilution values presented here are representative of the bulk fusion zone. A partially mixed zone (PMZ) will always exist adjacent to the fusion boundary due to the reduction of convective flow near the solid base metal. Within this zone, the composition varies from that of the base metal to that of the homogeneously mixed fusion zone. Once outside the PMZ, the fusion composition is known to be uniform.^[8] It has been demonstrated that the PMZ is generally very small in relation to the size of the homogeneously mixed fusion zone. For example, EPMA measurements conducted on welds prepared with both consumable and nonconsumable electrode processes^[8] have

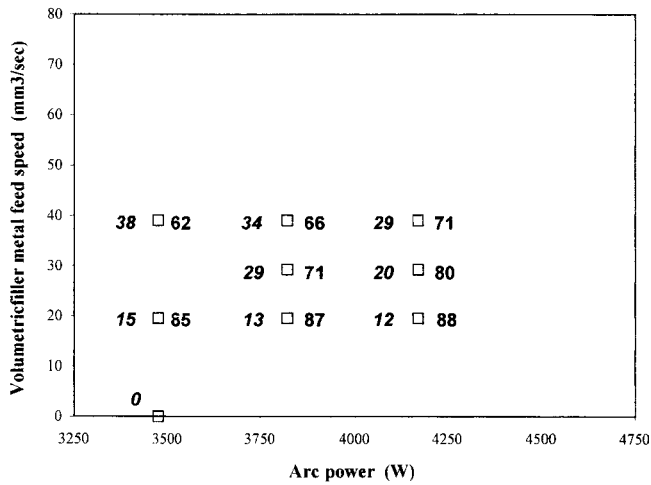


Fig. 6—Experimental matrix of fusion welds produced where IN622 was the substrate and AL-6XN was the filler metal. The numbers to the right signify the dilution level with respect to IN622 as the substrate, while those to the left are dilution levels with respect to AL-6XN as the substrate.

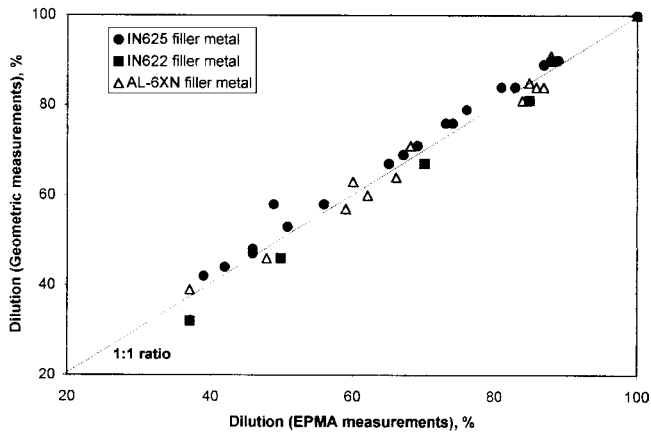


Fig. 7—Comparison plot of dilution levels as determined through both geometric measurements (using Eq. [3]) and chemical analysis (using Eq. [2]), showing good agreement between the two methods.

demonstrated that the PMZ is typically on the order of 75- to 150- μm wide. By comparison, the width and height of the fusion zone is typically on the order of several millimeters. Thus, the size of the PMZ is small compared to the size of the fusion zone. The presence of the PMZ may have a significant influence on corrosion performance in some applications, but this subject is not addressed in this work.

IV. DISCUSSION

Results from this work show that the dilution levels were directly related to the processing parameters of arc power and volumetric filler metal feed rate. By varying these two parameters, the relative volumetric melting rates of the filler metal and substrate were altered, which resulted in variable weld-metal dilutions. The observed trends are readily expected and can be interpreted based upon a simple power-balance dilution model proposed by DuPont and Marder.^[8] For a given set of welding parameters, the total amount of power available for melting the base and filler metals is a

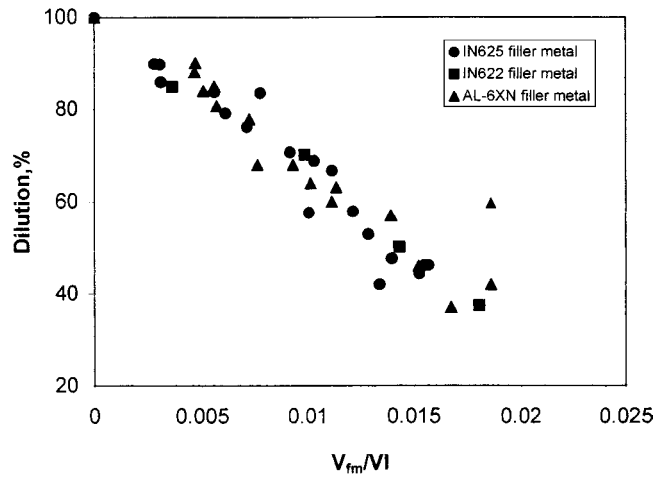


Fig. 8—Dilution level as a function of the ratio of volumetric filler metal feed rate to arc power.

fixed quantity, and a power balance across the arc can be written as

$$\eta_a \eta_m VI = V_{fm} E_{fm} + V_s E_s \quad [4]$$

where VI is the arc power; η_a and η_m are the arc and melting efficiencies, respectively; V_s is the volumetric melting rate of the substrate; and E_s and E_{fm} are the melting enthalpies of the substrate and filler metal, respectively. The quantity $\eta_a \eta_m VI$ is the melting power, and subsequently, the dilution level will change depending upon how this power is distributed between the filler metal and substrate. For example, with an increase in the volumetric filler-metal feed rate, which does not change the amount of power available for melting, as VI and V_{fm} are independent parameters, a larger portion of the total melting power is required to melt the larger volume of deposited filler metal. In this case, less power is available for melting the substrate, and the volumetric melting rate of the substrate decreases. Thus, the dilution levels decrease as the filler-metal feed rate increases, because a larger percentage of the fusion zone was composed of the filler metal. Conversely, the dilution levels are also altered by changing the amount of power available for melting through variation of the arc power. By decreasing the arc power while maintaining a fixed volumetric filler-metal feed rate, the total amount of power available for melting decreases. This again reduces the volumetric melting rate of the substrate, and, as a result, the dilution levels decrease with decreasing arc power. These trends are readily observed in the results shown in Figures 3 through 6, where, in terms of welding parameters, the dilution and resultant weld-metal composition are controlled by the volumetric filler-metal feed rate and melting power (which is controlled primarily by the arc power). In light of this, Figure 8 shows the dilution as a function of the ratio of the volumetric filler-metal feed rate to the arc power. It is interesting to note that the dilution data correlate very well to the V_{fm}/VI parameter. This can be understood by reference to the dilution model proposed by DuPont and Marder,^[8] as discussed subsequently.

A power balance across the arc can be used to express the dilution in terms of welding parameters (V and I), efficiency factors (η_a and η_m), and material thermal properties (E_s and E_{fm}).^[8] The final result is

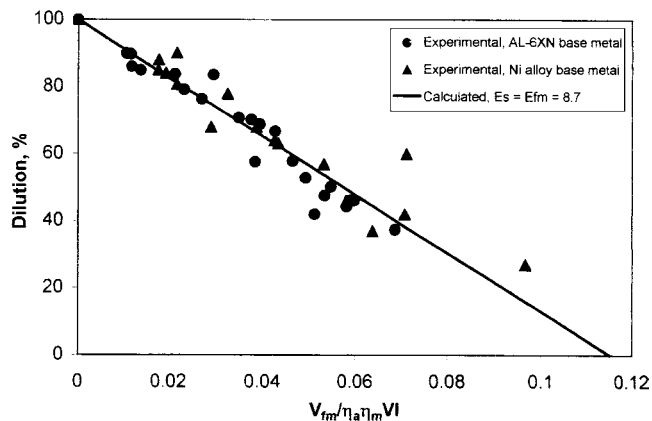


Fig. 9—Comparison of measured and calculated dilution levels as a function of the $V_{fm}/\eta_a\eta_m VI$ ratio.

$$D = \frac{1}{1 + \frac{V_{fm}E_s}{\eta_a\eta_m VI - E_{fm}V_{fm}}} \quad [5]$$

where D is the dilution (expressed as a fraction). This relationship can also be written as

$$D = \frac{1}{1 + \frac{E_s}{\frac{\eta_a\eta_m VI}{V_{fm}} - E_{fm}}} \quad [6]$$

Although Eq. [6] is simply an alternate form of the original Eq. [5], it is significant because it demonstrates that dilution depends only on the *ratio* of the volumetric filler-metal feed rate to the melting power, *i.e.*, the individual values of V_{fm} and $\eta_a\eta_m VI$ are not important. The difference between the arc power (as plotted in Figure 8) and melting power (as expressed in Eqs. [5] and [6]) lies within the arc-efficiency and melting-efficiency terms. It is well established that the arc efficiency is not sensitive to welding parameters,^[8] and, for the range of arc powers used here, η_a has a value of ~ 0.75 .^[8,9] The melting efficiency depends on the arc power and travel speed. For similar welding conditions utilized in this study, it has been shown^[8] that η_m varies only slightly from 0.2 to 0.4. Thus, the product of $\eta_a\eta_m$ in Eqs. [5] and [6] is expected to be fairly constant, and the arc power can be used as a reasonable representation of the available melting power. The scatter in the data is probably a result of slight variations in η_a and η_m that are not accounted for in the plot.

In further support of this, Figure 9 compares the measured and calculated dilution values as a function of the $V_{fm}/\eta_a\eta_m VI$ ratio using constant values of $\eta_a = 0.75$ and $\eta_m = 0.35$, and very good agreement is found between the calculated result and experimental data. Data is shown for both AL6XN and IN622/IN625 substrates. The calculated result requires knowledge of the substrate and filler-metal melting enthalpies. The melting enthalpy of austenitic stainless steel has been measured at 8.7 J/mm^3 ,^[10] but no melting enthalpy data could be found for IN622 or IN625. Based on available thermal data, no significant difference in melting enthalpy between the AL6XN and IN625/IN622 is expected. For example, available data on the temperature-dependent specific heat of 310 stainless steel^[11] (similar to AL6XN) and

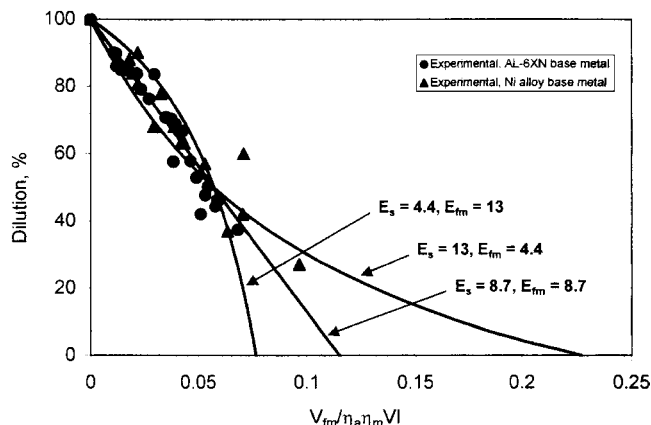


Fig. 10—Comparison of measured and calculated dilution levels as a function of the $V_{fm}/\eta_a\eta_m VI$ ratio using different values of E_{fm} and E_s .

IN625^[12] shows that their values are very similar. In addition, the melting enthalpy of pure Ni (9.8 J/mm^3)^[13] is not significantly different than that of austenitic stainless steel. It is also interesting to note that, within the range of dilution levels produced in this study, the substrate and filler-metal melting enthalpies are not expected to have a large influence on the dilution level. Support for this is provided in Figure 10, which shows the calculated dilution and experimental data as a function of the $V_{fm}/\eta_a\eta_m VI$ ratio for three different combinations of E_s and E_{fm} values: one in which $E_{fm} = E_s = 8.7 \text{ J/mm}^3$, and two other results in which E_s and E_{fm} were varied by 50 pct. Note that for dilution levels from ~ 40 to 100 pct dilution, that variations in E_{fm} and E_s have relatively little influence on the calculated dilution levels. The influence from the substrate and filler-metal melting enthalpies only becomes significant when the dilution level decreases below ~ 40 pct. This result is significant for two reasons. First, when the melting enthalpies of E_s and E_{fm} are similar, then dilution will vary linearly with the $V_{fm}/\eta_a\eta_m VI$ ratio. Deviation from linearity occurs when the melting enthalpies of the filler metal and substrate are different, and the deviation is most significant at low dilution levels. Second, from a practical perspective, the results show that at dilution levels above ~ 40 pct, the dilution level can be correlated almost exclusively to the $V_{fm}/\eta_a\eta_m VI$ ratio, because E_s and E_{fm} have a relatively small influence. This result is rather useful, because many welds are deposited within this dilution range in order to prevent lack of fusion. This effect probably accounts for the good agreement displayed between the experimental and calculated results shown in Figure 9. These relationships provide useful insight in elucidating the relative influences of material properties and welding parameters for control of weld-metal dilution and the resultant weld-metal composition.

V. CONCLUSIONS

A study was conducted in which fusion welds were prepared between a superaustenitic stainless steel (AL-6XN) and two Ni-based filler metals (IN625 and IN622). The effect of the processing parameters and materials properties on the final fusion-zone composition was investigated, and the following results were observed.

1. The processing parameters of arc power and filler-metal

feed rate were found to have a direct influence on the resultant weld-metal dilution. Altering these welding parameters lead to changes in the volumetric melting rates of the filler metal and substrate, which resulted in varying dilution levels of the welds. The dilution levels were found to decrease with a decrease in arc power and/or increase in volumetric filler-metal feed rate.

2. A previous dilution model was used to demonstrate that the dilution level depends only on the *ratio* of the volumetric filler-metal feed rate to the melting power, *i.e.*, the individual values of V_{fm} and $\eta_a \eta_m VI$ are not important.
3. Within the rather large range of parameters investigated here, η_a and η_m are not expected to vary significantly, and the dilution level could, thus, be correlated to the V_{fm}/VI ratio.
4. The melting enthalpy of the substrate and filler metal does not have a large influence on the dilution at dilution levels from ~40 to 100 pct.

ACKNOWLEDGMENTS

The authors gratefully acknowledge financial support for this work provided by the Office of Naval Research under Contract No. N00014-99-1-0887. Technical discussions with George Yoder, ONR, throughout the course of the work are also gratefully acknowledged.

REFERENCES

1. J.F. Grubb and J.R. Maurer: *Corrosion 1995*, Orlando, FL, The NACE Annual Conf., paper no. 300.
2. K. Sugimoto and Y. Sawada: *Corr. Sci.*, 1977, vol. 17, pp. 425-45.
3. M.W. Tan, E. Akiyama, A. Kawashima, K. Asami, and K. Hashimoto: *Corr. Sci.*, 1995, vol. 37, pp. 1289-95.
4. I. Olefjord, B. Brox, and U. Jelvestam: *J. Electrochem. Soc.*, 1985, vol. 132 (12), pp. 2854-61.
5. C.D. Lundin, E. Liu, G. Zhou, and C.Y. Qiao: Welding Research Council Bulletin No. 428, WRC, New York, NY, Jan. 1998.
6. K.K. Baek, H.J. Sung, C.S. Im, C.S., I.P. Hong, and D.K. Kim: *Corrosion 1998*, The NACE Annual Conference, paper no. 474.
7. J.I. Goldstein, D.E. Newbury, P. Echlin, Joy, A.D. Romig, Jr., C.E. Lyman, C. Fiori, and E. Lifshin: *Scanning Electron Microscopy and X-ray Microanalysis*, 2nd ed., Plenum Press, New York, NY, 1992, p. 405.
8. J.N. DuPont and A.R. Marder: *Metall. Mater. Trans. B*, 1996, vol. 27B, pp. 481-89.
9. P.W. Fuerschbach and G.A. Knorovsky: *Welding J.*, 1991, vol. 70 (1), pp. 287s-297s.
10. L. Leibowitz: *Properties for LMFBR Safety Analysis*, ANL-CEN-RSD-76-1, Argonne National Laboratory, Argonne, IL, 1976.
11. D. Peckner and I.M. Bernstein: *Handbook of Stainless Steels*, McGraw-Hill Book Company, New York, NY, 1977, pp. 19-26.
12. Inconel Alloys Publication No. IAI-83, INCO Alloys International, Huntington, WV, 1991, p. 3.
13. K.K. Kelley: *Contributions to the Data on Theoretical Metallurgy*, U.S. Bureau of Mines Bulletin No. 584, U.S. Government Printing Office, Washington, DC, 1960.